A Kinetic Study of Wild-Type and Mutant Dihydrofolate Reductases from *Lactobacillus casei*

J. Andrews,*,‡ C. A. Fierke,§,‖ B. Birdsall,⊥ G. Ostler,⊥ J. Feeney,⊥ G. C. K. Roberts,# and S. J. Benkovic*,§,○

Department of Chemistry, The Pennsylvania State University, University Park, Pennsylvania 16802, Department of Pharmacy, University of Manchester, Manchester M13 9PL, U.K., Physical Biochemistry Division, NIMR, Mill Hill, London NW7 1AA, U.K., and Department of Biochemistry, University of Leicester, University Road, Leicester LE1 7RH, U.K.

Received January 3, 1989; Revised Manuscript Received March 30, 1989

ABSTRACT: A kinetic scheme is presented for *Lactobacillus casei* dihydrofolate reductase that predicts steady-state kinetic parameters. This scheme was derived from measuring association and dissociation rate constants and pre-steady-state transients by using stopped-flow fluorescence and absorbance spectroscopy. Two major features of this kinetic scheme are the following: (i) product dissociation is the rate-limiting step for steady-state turnover at low pH and follows a specific, preferred pathway in which tetrahydrofolate (H_4F) dissociation occurs after NADPH replaces $NADP^+$ in the ternary complex; (ii) the rate constant for hydride transfer from NADPH to dihydrofolate (H_2F) is rapid (k_{hyd} = 430 s^{-1}), favorable (K_{eq} = 290), and pH dependent (pK_a = 6.0), reflecting ionization of a single group. Not only is this scheme identical in form with the *Escherichia coli* kinetic scheme [Fierke et al. (1987) *Biochemistry 26*, 4085] but moreover none of the rate constants vary by more than 40-fold despite there being less than 30% amino acid homology between the two enzymes. This similarity is consistent with their overall structural congruence. The role of Trp-21 of *L. casei* dihydrofolate reductase in binding and catalysis was probed by amino acid substitution. Trp-21, a strictly conserved residue near both the folate and coenzyme binding sites, was replaced by leucine. Two major effects of this substitution are on (i) the rate constant for hydride transfer which decreases 100-fold, becoming the rate-limiting step in steady-state turnover, and (ii) the affinities for NADPH and $NADP^+$ which decrease by ≈3.5 and ≈0.5 kcal mol^{-1}, respectively. These results are consistent with high-resolution NMR spectroscopy studies [Birdsall et al. (1989) *Biochemistry 28*, 1353] suggesting the major structural effects of W21L mutant are on binding of the nicotinamide moiety of the coenzyme.

Dihydrofolate reductase (5,6,7,8-tetrahydrofolate:$NADP^+$ oxidoreductase, EC 1.5.1.3) catalyzes the NADPH-dependent reduction of 7,8-dihydrofolate (H_2F)[1] to 5,6,7,8-tetrahydrofolate (H_4F). This enzyme is necessary for maintaining intracellular pools of H_4F and its derivatives which are essential cofactors in the one-carbon-transfer reactions utilized in the biosynthesis of purines, thymidylate, and several amino acids. In addition, it is the target enzyme for antifolate drugs such as the antineoplastic drug methotrexate (MTX) and the antibacterial drug trimethoprim (TMP). Because of its biological and pharmacological importance, dihydrofolate reductase (DHFR) has been the subject of intensive structural and kinetic studies. For example, the structures of the *Escherichia coli*, *Lactobacillus casei*, and chicken liver enzymes have been determined to 1.7 Å for some binary and ternary complexes (Bolin et al., 1982; Filman et al., 1982; Matthews et al., 1985). High-resolution NMR spectroscopy has been used to study complexes of the *L. casei*, wild-type DHFR, and single-site mutants (W21L and D26E) with substrates, substrate analogues, and coenzymes (Birdsall et al., 1989). In addition, a complete kinetic scheme for wild-type *E. coli* DHFR has been derived from pre-steady-state and steady-state kinetics (Fierke et al., 1987). Despite knowledge of the kinetics and the identities of the amino acids at the active site of DHFR, the function of many of these amino acids in binding and catalysis is unclear. Site-directed mutagenesis of the *E. coli* DHFR combined with detailed kinetic analysis has been utilized to establish structure–function relationships (Mayer et al., 1986; Howell et al., 1985, 1987; Chen et al., 1987; Benkovic et al., 1988, 1989; Fierke & Benkovic, 1989). In the present work, we determine a complete kinetic scheme for wild-type *L. casei* DHFR for comparison with the *E. coli* scheme, in order to probe the effect of multiple amino acid changes on function. In addition, the kinetics of the W21L mutant have been investigated and related to the structural changes observed by NMR in order to establish the role of this conserved residue in binding and catalysis.

Materials and Methods

Ligands. 7,8-Dihydrofolate (H_2F) was prepared from folic acid by the method of Blakley (1960). (6*S*)-Tetrahydrofolate (H_4F) was prepared from H_2F by using dihydrofolate reductase (Mathews & Huennekens, 1960) and purified on DE-52 resin eluting with a triethylammonium bicarbonate linear gradient (Curthoys et al., 1972). Folate was purified by treatment with activated charcoal followed by elution off a phosphocellulose column with 0.1 M K_2HPO_4. Trimethoprim and methotrexate were purchased from Sigma Chemical Co. [4′(*R*)-^{2}H]NADPH and thioNADPH (TNADPH) were prepared by using *Leuconostoc mesenteroides* alcohol dehydrogenase (Stone & Morrison, 1982) obtained from Re-

* Authors to whom correspondence should be addressed.
‡ University of Manchester.
§ The Pennsylvania State University.
‖ Present address: Department of Biochemistry, Duke University Medical Center, Durham, NC 27710.
⊥ NIMR.
University of Leicester.
○ Supported by NIH Grant GM24129.

[1] Abbreviations: H_2F, 7,8-dihydrofolate; H_4F, 5,6,7,8-tetrahydrofolate; DHFR, dihydrofolate reductase; MTX, methotrexate; TMP, trimethoprim; NADPH, NH, nicotinamide adenine dinucleotide phosphate, reduced; $NADP^+$, N, nicotinamide adenine dinucleotide phosphate; Fol, folate; W21L, tryptophan-21 → leucine DHFR mutant; TNADPH, thionicotinamide adenine dinucleotide phosphate; D26E, aspartic acid-26 → glutamic acid DHFR mutant.

0006-2960/89/0428-5743$01.50/0

search Plus, Inc. NADPH, TNADPH, and $NADP^+$ were purified by FPLC on a Mono Q column using a salt gradient (Orr & Blanchard, 1984). This procedure removes impurities which have been found to inhibit *L. casei* DHFR turnover at low pH.

The concentrations of the ligands were determined spectrophotometrically by using the following extinction coefficients: H_2F, 28 000 M^{-1} cm^{-1} at 282 nm, pH 7.4 (Dawson et al., 1969); H_4F, 28 000 M^{-1} cm^{-1} at 297 nm, pH 7.5 (Kallen & Jencks, 1966); folic acid, 27 600 M^{-1} cm^{-1} at 282 nm, pH 7.0 (Rabinowitz, 1960); TMP, 6060 M^{-1} cm^{-1} at 271 nm in 0.1 M acetic acid (Roth & Strelitz, 1969); MTX, 22 100 M^{-1} cm^{-1} at 302 nm in 0.1 M KOH (Seeger et al., 1949); NADPH, 6200 M^{-1} cm^{-1} at 339 nm, pH 7.5; and $NADP^+$, 18 000 M^{-1} cm^{-1} at 259 nm, pH 7.0 (P-L Biochemicals, 1961). The concentration of H_4F was also determined enzymatically by using a molar absorbancy change for the 10-formyl-H_4F synthetase reaction of 12 000 M^{-1} cm^{-1} at 312 nm (Smith et al., 1981). The concentration of H_2F or NADPH was also determined enzymatically by using a molar absorbancy change for the dihydrofolate reductase reaction of 11 800 M^{-1} cm^{-1} at 340 nm (Stone & Morrison, 1982).

(*A*) *DHFR.* The *L. casei* DHFR gene was cloned into *E. coli* and fully sequenced as described by Andrews et al. (1985). The W21L mutant was made by oligonucleotide-directed mutagenesis using a modification of the gapped duplex method originally developed by Kramer et al. (1984). The bacterial cells were grown, and the proteins were purified as described by Birdsall et al. (1988). The enzyme concentrations were determined by either MTX titration (Dann et al., 1976; Williams et al., 1979) or spectrophotometrically at 280 nm by using a molar extinction coefficient of 30 500 M^{-1} cm^{-1} for wild type or 23 500 M^{-1} cm^{-1} for W21L. Both proteins were shown to be homogeneous by the presence of a single band on an SDS–polyacrylamide gel.

Kinetics. All measurements were performed at 25 °C in a buffer containing 50 mM 2-(*N*-morpholino)ethanesulfonic acid, 25 mM tris(hydroxymethyl)aminomethane, 25 mM ethanolamine, 500 mM potassium chloride, 1 mM ethylenediaminetetraacetate, and 1 mM dithioerythritol (KMB buffer). The ionic strength of this buffer remains constant over the pH range used (Ellis & Morrison, 1982). Additionally, in some cases the buffer was purged with argon. The buffer used with *E. coli* DHFR (MTEN) is the same as KMB buffer except that 100 mM sodium chloride replaces 500 mM potassium chloride.

(*A*) *Steady-State Kinetics.* Initial velocities for dihydrofolate reductase reactions were determined by measuring the rate of either the enzyme-dependent decrease in H_2F and NADPH or, in the reverse direction, the increase in H_2F and NADPH at 340 nm (Fierke et al., 1987) using a molar absorbancy change of 11 800 M^{-1} cm^{-1} (Stone & Morrison, 1982). DHFR was preincubated with NADPH or $NADP^+$ before initiating turnover in order to remove hysteretic behavior (Penner & Frieden, 1985).

Data obtained by varying the substrate concentration were fitted to eq 1 (using an RS1 statistical program) to yield values for the steady-state kinetic parameters k_{cat} and k_{cat}/K_M. The values obtained at different pH values were then fitted to eq 2 where y represents the value of k_{cat} or k_{cat}/K_M at a particular pH value, C represents the pH-independent value of the parameter, and K_A is an acid dissociation constant.

$$v = k_{cat}[S]/(K_M + [S]) \quad (1)$$

$$y = C/(1 + K_A/[H^+]) \quad (2)$$

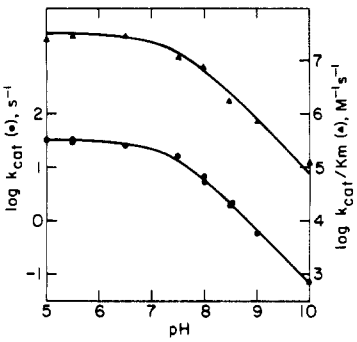

FIGURE 1: Variation with pH of log k_{cat} and log $[k_{cat}/K_M(H_2F)]$ for the reaction catalyzed by wild-type *L. casei* dihydrofolate reductase in KMB buffer, 25 °C. The lines represent a best fit to eq 1 with the parameters given in Table I.

(*B*) *Transient Kinetics.* Association and dissociation rate constants and pre-steady-state kinetic data were obtained by using a stopped-flow apparatus built in the laboratory of Johnson (1986), operating in either a fluorescence or a transmittance mode, with a 1.6-ms dead time, a 2-mm sample cell, and a thermostated sample cell. Interference filters (Corion Corp.) were used on both the excitation and emission sides. In most cases, the formation of an enzyme–substrate complex was followed by using a 290-nm interference filter for excitation and then monitoring either the quenching of the intrinsic enzyme fluorescence with a 340-nm filter on the emission side or the enhancement of coenzyme fluorescence with a 450-nm filter (Lackowicz, 1983; Velick, 1958; Dunn & King, 1980). Transmittance measurements were made by using a 340-nm excitation filter and were later converted to absorbance. A molar absorbancy change for the chemical reaction of 8500 M^{-1} cm^{-1} using the 340-nm band-pass filter was determined at low enzyme concentration (Fierke et al., 1987). For slow reactions, a neutral density filter (0.2–2.0 OD) was placed in this excitation beam to decrease the light intensity and thus decrease photobleaching of the sample. In most experiments, the average of at least four runs was used for data analysis.

Data were collected by a computer over a given time interval following a trigger impulse. All data were analyzed by using an iterative, nonlinear least-squares fit computer program using a modification of the method of moments (Dyson & Isenberg, 1971; Johnson, 1986). Kinetic data were analyzed with either a single exponential, a double exponential, or a single exponential followed by a linear rate. The data were then transferred to a Vax microcomputer where a fit to more complicated models was tested by using the computer program KINSIM (Barshop et al., 1983). This latter method was used to estimate the rate constant for hydride transfer at various pH values.

Binding Constants. The binding of ligands to wild-type and mutant DHFR was measured fluorometrically at 25 °C using the methods previously described (Birdsall et al., 1978, 1983). The solutions contained 0.1–4.0 μM enzyme in 500 mM KCl and 15 mM Bis-Tris, pH 6.0.

RESULTS

Steady-State Kinetic Parameters. Values for k_{cat} and k_{cat}/K_M for H_2F and folate were determined by varying substrate concentrations (1–50 μM) at 50 μM NADPH. Those parameters were determined as a function of pH for wild-type *L. casei* DHFR (Figure 1) and W21L DHFR (H_2F only). These k_{cat} values are larger than previously measured (Dann et al., 1976) because repurified NADPH was used in the present work. The use of unpurified NADPH generates the

Table I: Steady-State Kinetic Parameters[a]

substrate	enzyme	parameter	pH-independent value	pK_a	isotope effect
H_2F	wild type	k_{cat} (s^{-1})	31 ± 2	7.33 ± 0.1	1.14 ± 0.11 (pH 5); 2.7 ± 0.3 (pH 9)
		k_{cat}/K_M (M^{-1} s^{-1} × 10^{-7})	3.0 ± 0.5	7.4 ± 0.1	1.4 ± 0.4 (pH 5); 3.9 ± 1 (pH 9)
H_2F	wild type[b]	k_{cat} (s^{-1})	32.5	7.12	1.18 (pH 5); 2.98 (pH 9)
		k_{cat}/K_M (M^{-1} s^{-1} × 0^{-7})	1.4	7.35	1.10 (pH 5); 2.96 (pH 9)
H_2F	W21L	k_{cat} (s^{-1})	4.3 ± 0.7	5.85 ± 0.1	2.5 ± 0.4 (pH 5.5)
		k_{cat}/K_M (M^{-1} s^{-1} × 10^{-6})	5 ± 1	5.1 ± 0.2	1.9 ± 0.5 (pH 5.5)
folate	wild type	k_{cat} (s^{-1})	0.074 ± 0.01	6.9 ± 0.1	5.1 ± 0.9 (pH 5)
		k_{cat}/K_M (M^{-1} s^{-1} × 10^{-4})	5 ± 1	5.6 ± 0.1	1.5 ± 0.5 (pH 5)

[a] 50 μM NADPH (wild type) and 100 μM NADPH, saturating (W21L) KMB buffer, 25 °C. [b] Calculated from steady-state kinetic expressions and Schemes III and IV as described under Discussion.

Table II: Kinetic Binding Constants: Relaxation Method

ligand	enzyme species	k_{on} × 10^{-6} (M^{-1} s^{-1})			k_{off} (s^{-1})		
		L. casei[a]	W21L[a]	*E. coli*[b]	*L. casei*[a]	W21L	*E. coli*[b]
NADPH	E	14 ± 1	12 ± 2	20	≤2	35 ± 5	3.5
	E·H_4F	12 ± 2		8	10 ± 5		85
$NADP^+$	E	9 ± 2		13	85 ± 15		295
	E·Fol	6.7 ± 0.6			20 ± 6		
	E·H_4F	10 ± 2			290 ± 30		
TNADPH[c]	E·H_2F	12 ± 3			20 ± 10		
H_2F	E	14 ± 2	3.2 ± 0.3	42	5 ± 3	5.8 ± 1	47
H_4F	E	16 ± 2	6 ± 1	24	3 ± 2.5	4 ± 2	<2
	E·NADPH	12 ± 2	12 ± 2	2	35 ± 15	70 ± 20	5
folate[c]	E	8 ± 1.5			112 ± 12		
	E·$NADP^+$	9 ± 1.5			52 ± 8		

[a] Measured in 50 mM MES, 25 mM ethanolamine, 25 mM Tris, and 500 mM KCl, pH 6.5, 25 °C. [b] Measured in 50 mM MES, 25 mM ethanolamine, 25 mM Tris, and 100 mM NaCl, pH 6.0, 25 °C (Fierke et al., 1987). [c] TNADPH and folate are poor substrates for *L. casei* DHFR (Hyde, 1981).

Scheme I

$$E_2 \underset{k_{-2}}{\overset{k_2}{\rightleftharpoons}} E_1 + L_1 \underset{k_{off}}{\overset{k_{on}}{\rightleftharpoons}} E_1 \cdot L_1 + L_2 \underset{k_{off}'}{\overset{k_{on}'}{\rightleftharpoons}} E_1 \cdot L_1 \cdot L_2$$

same behavior as reported earlier, so there is no discernible difference between cloned and native DHFR proteins. The identity of the inhibitor was not pursued. As illustrated in Figure 1, in each of these reactions the steady-state kinetic parameters increase as the pH decreases and then reach a plateau at low pH, suggesting that protonation of some residue is necessary to achieve maximum velocity, as observed for *E. coli* DHFR (Stone & Morrison, 1984). Analysis of the k_{cat} and k_{cat}/K_M profiles in terms of a single pK_a value gives satisfactory fits and yields the values shown in Table I. Also included in this table are the deuterium isotope effects on k_{cat} and k_{cat}/K_M for wild-type and W21L determined by using saturating [4′(*R*)-^{2}H]NADPH.

The rate of the reverse reaction (net conversion of H_4F and $NADP^+$ to form H_2F and NADPH) was measured from the increase in absorbance at 340 nm in a reaction mixture containing 240 μM H_4F, 2 mM $NADP^+$, and KMB buffer, pH 10, 25 °C. The observed rate of these reactions was virtually unaffected when the concentration of either substrate was doubled, implying that both substrates are saturating. Values of 1.5 ± 0.3 s^{-1} (wild type) and 0.015 ± 0.002 s^{-1} (W21L) for k_{cat} were obtained.

Binding Kinetics Relaxation Method. The rate constants for binding ligands to DHFR in either the cofactor or the substrate binding sites can be measured by following the quenching of the intrinsic enzyme fluorescence due predominantly to its tryptophan residues. In the formation of binary complexes of DHFR at saturating substrate concentration, two exponentials were observed, a rapid phase whose rate was dependent on ligand concentration followed by a ligand-independent phase, while in the formation of ternary complexes (by addition of a ligand to the binary complex) a single ligand-dependent exponential is observed (Dunn et al., 1978; Dunn & King, 1980; Cayley et al., 1981). Cayley et al. (1981) concluded that this behavior is due to the mechanism shown in Scheme I, where substrate binds rapidly to only one of two conformers of the free enzyme and interconversion between conformers is slow. Similar behavior has now been observed for the W21L mutant.

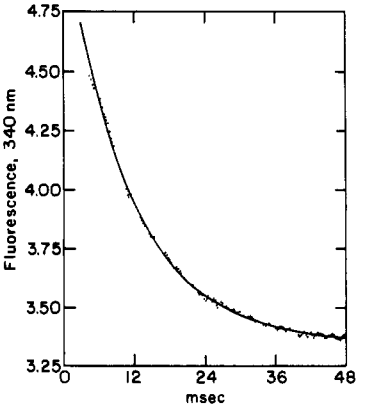

FIGURE 2: Measurement of the rate of binding NADPH to wild-type *L. casei* DHFR by diluting enzyme 2-fold into NADPH (final conditions: 0.5 μM DHFR, 6 μM NADPH, and KMB buffer, pH 6.5, 25 °C) and observing fluorescence quenching at 340 nm due to formation of the E·NADPH complex. The data are fitted by a single-exponential decay.

Figure 2 illustrates the rapid phase of the decrease in tryptophan fluorescence at 340 nm when wild-type *L. casei* DHFR is mixed with NADPH. This fluorescence change is well fitted by a single exponential with a rate constant of 89 ± 5 s^{-1}. The apparent first-order rate constant increases linearly with the ligand concentration over this NADPH range (1–10 μM), showing no sign of saturation as observed for *E. coli* DHFR (Fierke et al., 1987). For a simple association reaction, the observed rate constant under pseudo-first-order conditions may be approximated by $k_{obsd} = k_{on}[L] + k_{off}$ where k_{on} and k_{off} are the association and dissociation rate constants,

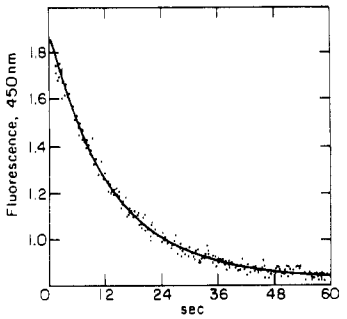

FIGURE 3: Measurement of the dissociation rate constant, k_{off}, for NADPH obtained by diluting the E·NADPH binary complex 2-fold into NADP$^+$ (final conditions: 2 μM DHFR, 10 μM NADPH, 1 mM NADP$^+$, and KMB buffer, 25 °C) and observing the decrease in the fluorescence energy transfer (excitation, 290 nm; emission, 450 nm) due to formation of the E·NADP$^+$ binary complex. The data are fitted by a single-exponential decay.

Table III: Dissociation Rate Constants: Competition Method

ligand	enzyme species	trapping ligand	k_{off} (s^{-1})		
			L. casei[a]	W21L[a]	*E. coli*[b]
NADPH	E·NADPH	NADP$^+$	0.09 ± 0.03	26 ± 5	3.6
	E·H_4F·NADPH	NADP$^+$	8 ± 2		85
	E·Fol·NADPH	NADP$^+$	0.5 ± 0.1		
NADP$^+$	E·NADP$^+$	NADPH	85 ± 10	330 ± 30	290
	E·Fol·NADP$^+$	NADPH	16 ± 4		
H_2F	E·H_2F	MTX	3.7 ± 1.3	6.8 ± 1	22
	E·H_2F·TNADPH	MTX	22 ± 6		43
H_4F	E·H_4F	MTX	0.5 ± 0.05	4.2 ± 0.2	1.4
	E·H_2F·NADPH	MTX, TMP	40 ± 8	65 ± 10	12
	E·H_4F·NADP$^+$	MTX	1.7 ± 0.2		2.4
Fol	E·Fol	MTX	130 ± 20		
	E·Fol·NADP$^+$	MTX	55 ± 8		

[a] Same conditions as Table II. [b] Taken from Fierke et al. (1987).

respectively. Thus, in a linear plot of k_{obsd} vs [L], the slope is k_{on} and the intercept is k_{off}. Using these assumptions, we measured the association rate constants for binding a variety of ligands to both free enzyme and binary complexes of *L. casei* wild-type and W21L DHFR at pH 6.5, KMB buffer, 25 °C, and are listed in Table II. Corresponding rate constants for *E. coli* DHFR are included in this table.

Competition Experiments. The dissociation rate constant of a ligand from DHFR can also be measured by a competition experiment (Birdsall et al., 1980). In this technique, the enzyme–ligand complex (E·L_1) is mixed with a large excess of a second ligand which competes for the binding site (see Scheme II), and the formation of the new enzyme–ligand complex (E·L_2) is monitored by a fluorescence change due to the difference in fluorescence quenching by the two ligands. When $k_1[L_1] \ll k_2[L_2] \gg k_{-1}$, then k_{obsd} for this reaction is equal to k_{-1}, the dissociation rate constant for L_1. The validity of these conditions can be checked by showing that k_{obsd} is independent of the concentration of L_2. Figure 3 shows the measurement of the dissociation rate constant of NADPH from DHFR by mixing the enzyme–NADPH complex with NADP$^+$ and observing a time-dependent decrease in the fluorescence signal. The rate constant for this reaction is independent of the concentration of NADPH, NADP$^+$, and DHFR. Dissociation rate constants determined by using this technique for a variety of ligands are shown in Table III for *L. casei*, W21L, and *E. coli* DHFR.

Scheme II

$$E\cdot L_1 \underset{k_1}{\overset{k_{-1}}{\rightleftharpoons}} E + L_1$$

$$E + L_2 \underset{k_{-2}}{\overset{k_2}{\rightleftharpoons}} E\cdot L_2$$

Table IV: Comparison of Equilibrium and Kinetic Binding Constants

	k_{off}/k_{on} (LC)[d] (μM)	K_D (LC)[a] (μM)	K_D (W21L)[a] (μM)	K_D (EC)[e] (μM)
NADPH	0.006 ± 0.003	0.01[b]	4.2 ± 0.2	0.33
NADP$^+$	9 ± 3	17.3[b]	34 ± 6	24
H_2F	0.26 ± 0.13	0.44[c]		0.22
folate	14 ± 5	9 ± 2	28 ± 3	

[a] Measured in 15 mM Bis-Tris and 500 mM KCl, pH 6.0, 25 °C (not calculated as in *d*). [b] Taken from Birdsall et al. (1980). [c] Measured in 50 mM triethanolamine and 100 mM KCl, pH 6.0, 20 °C. [d] Calculated by using k_{on} from Table II and k_{off} from Table III. Measured in KMB buffer, pH 6.5, 25 °C. [e] Taken from Fierke et al. (1987). Measured in MTEN buffer, pH 6, 25 °C.

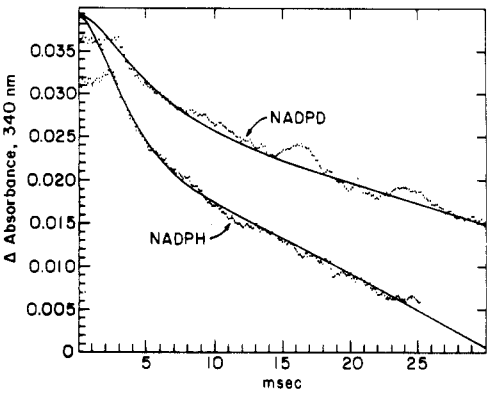

FIGURE 4: Measurement of the pre-steady-state burst by stopped-flow absorbance spectroscopy. DHFR is preincubated with NADPH or [4′(*R*)-^{2}H]NADPD, and the reaction is initiated by addition of H_2F. Final conditions are 2.2 μM *L. casei* DHFR, 20 μM NADPH(D), 50 μM H_2F, and KMB buffer, pH 5.5, 25 °C. The solid line is simulated by the computer program KINSIM (Barshop & Frieden, 1983) using the rate constants shown in Scheme III except for $^Hk_{hyd}$ = 320 s^{-1} (H) and $^Dk_{hyd}$ = 120 s^{-1} (D) at pH 5.5.

The results for the binding rate constants show that the assumption of a simple association step for the ligand-dependent step is reasonable. First, the dissociation rate constants measured by the two techniques, relaxation and competition, are identical within experimental error, showing that there is no slow isomerization following association. Second, the relationship between the ratio k_{off}/k_{on} and the association constant, K_D, depends on the equilibrium between two enzyme conformations (Scheme I) where $K_{eq} \approx 1$ at pH 6.5 (Dunn et al., 1978). Consequently, the measured K_D should be 2-fold larger than the ratio of k_{off}/k_{on} (eq 3). As shown in Table IV, this is true for the binding of NADPH, NADP$^+$, and H_2F whereas the K_D for folate is slightly smaller than predicted.

$$K_D = (k_{off}/k_{on})[(K_{eq} + 1)/K_{eq}] \quad (3)$$

Pre-Steady-State Experiments. The rate constant for hydride transfer from NADPH to H_2F can be determined from the rate constant and amplitude of a burst of product formation measured in pre-steady-state experiments, as described for *E. coli* DHFR (Fierke et al., 1987). *L. casei* DHFR was preincubated with NADPH or NADPD and diluted 2-fold into a H_2F solution to initiate the reaction which was monitored by a decrease in absorbance (using a 340-nm filter) due to the disappearance of NADPH/NADPD and H_2F as shown in Figure 4. From a comparison of the NADPH and NADPD data, it is apparent that there is an isotope effect on the burst rate constant and a smaller effect on the turnover rate. When these data are fitted by the simple model of a single-exponential decay followed by a linear rate process, the observed kinetic parameters are as follows: k_{burst} = 300 ± 30 s^{-1} (H),

Scheme III: Kinetic Scheme for *L. casei* Dihydrofolate Reductase in KMB Buffer, pH 6.5, 25 °C[a]

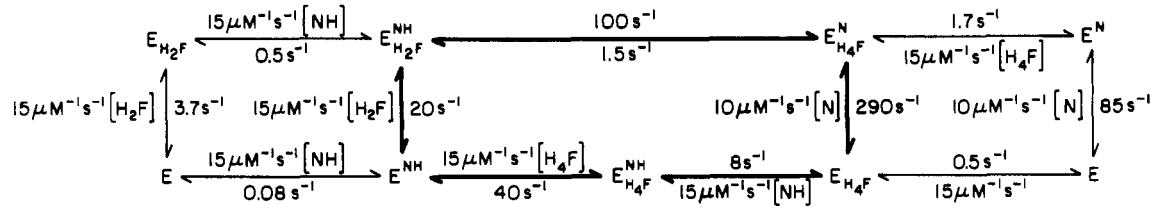

[a] The heavy arrows indicate the kinetic pathway for steady-state turnover at saturating substrate conditions. N, $NADP^+$; NH, NADPH; H_2F, dihydrofolate; H_4F, tetrahydrofolate.

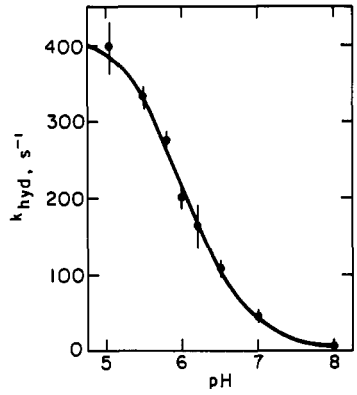

FIGURE 5: Observed rate constant for hydride transfer catalyzed by *L. casei* DHFR as a function of pH. The rate constant for hydride transfer is calculated by using KINSIM and Scheme III as described in the text. The solid line is fitted to the equation $k_{obsd} = k_{hyd}/(1 + K_a/[H^+])$ where $k_{hyd} = 430 \pm 30\ s^{-1}$ and $pK_a = 6.0 \pm 0.1$.

$110 \pm 10\ s^{-1}$ (D); $amp_{burst}/[E] = 0.8 \pm 0.1$ (H), 0.5 ± 0.1 (D); and $k_{cat} = 30 \pm 1\ s^{-1}$ (H), $25 \pm 1\ s^{-1}$ (D). The rate constant for hydride transfer (k_{hyd}) was estimated by using the computer simulation program KINSIM (Barshop et al., 1983) with the kinetic scheme shown in Scheme III to provide the best fit of the observed pre-steady-state data. All of the rate constants in this scheme except that for hydride transfer from NADPH to H_2F were determined independently. The simulated curves shown in Figure 4 were determined with KINSIM using $^Hk_{hyd} = 320 \pm 20\ s^{-1}$ and $^Dk_{hyd} = 110 \pm 10\ s^{-1}$, indicating that the intrinsic deuterium isotope effect is 2.9 ± 0.5, consistent with the steady-state isotope effect at high pH.

To determine the rate constant for hydride transfer from the protonated ternary complex ($H{\cdot}E{\cdot}NH{\cdot}H_2F$) and the intrinsic pK_a of this complex, we measured the pH dependence of the observed hydride transfer rate constant as shown in Figure 5. When these data are fitted to a single pK_a, the pH-independent rate constant for hydride transfer is calculated to be $k_{hyd} = 430 \pm 30\ s^{-1}$, and the pK_a of the ternary complex is 6.0 ± 0.1.

Discussion

Summary of Overall Kinetic Scheme for Wild-Type DHFR. From the data presented under Results, it is possible to construct a complete kinetic scheme for *L. casei* DHFR-catalyzed reduction of H_2F at pH 6.5 as shown in Scheme III. The heavy arrows indicate the preferred kinetic pathway for steady-state turnover under saturating conditions. The association and dissociation rate constants for the formation of all binary complexes and the formation of the ternary complexes, $E{\cdot}N{\cdot}H_4F$ and $E{\cdot}NH{\cdot}H_4F$, were measured directly. Direct measurement of the association and dissociation rate constants for the formation of the substrate ternary complex, $E{\cdot}NH{\cdot}H_2F$, is impossible as this complex is reactive. Since folate and TNADPH (Hyde, 1981) are poor substrates for this enzyme, they were used as analogues of H_2F and NADPH in order to estimate the association and dissociation rate constants for formation of $E{\cdot}NH{\cdot}H_2F$. The enzyme-catalyzed rate constant for hydride transfer from NADPH to H_2F at pH 6.5 was measured from pre-steady-state experiments (Figure 5). The rate constant for hydride transfer in the reverse direction (H_4F to $NADP^+$) was estimated to be $1.5\ s^{-1}$ from the observed steady-state rate constant in this direction at pH 10 with saturating substrates. Hydride transfer is the main rate-limiting step under these conditions since it is rate limiting in the forward direction at high pH ($^Hk_{cat}/^Dk_{cat} \approx 3.0$) and the kinetically significant product (NADPH and H_2F) dissociation rate constants are fast (H_2F from $E{\cdot}NH{\cdot}H_2F$, $20\ s^{-1}$; NADPH from $E{\cdot}NH{\cdot}H_4F$, $8\ s^{-1}$). Since the rate for H_2F dissociation is greater than that for NADPH in this direction from the ternary product complex, $E{\cdot}NH{\cdot}H_2F$ (20 vs $0.5\ s^{-1}$), this complex would primarily partition along a pathway rapidly leading to $E{\cdot}H_4F$ through $E{\cdot}NH{\cdot}H_4F$ and avoiding formation of an abortive $E{\cdot}N{\cdot}H_2F$ complex. Consequently, the measurement of initial rates should reflect the chemical step.

Scheme IV: pH Independence Kinetic Scheme for *L. casei* Dihydrofolate Reductase in KMB Buffer, 25 °C[a]

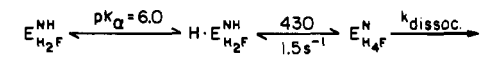

[a] Abbreviations: N, $NADP^+$; NH, NADPH; H_2F, dihydrofolate; H_4F, tetrahydrofolate.

The pH dependence of this scheme is illustrated in Scheme IV. A single pK_a of 6.0 ± 0.1 is observed in the pre-steady-state which is the pK_a for the $E{\cdot}NH{\cdot}H_2F$ complex. The rate constant for hydride transfer from the protonated ternary complex, $H{\cdot}E{\cdot}NH{\cdot}H_2F$, is calculated to be $430 \pm 30\ s^{-1}$. In this study, there is no evidence for slow ($<500\ s^{-1}$) proton transfer between either enzyme and solvent or enzyme and H_2F.

A good test of the validity of Schemes III and IV is a comparison of the measured steady-state parameters with those predicted from this model as shown in Table I. Steady-state kinetic parameters for the proposed schemes (Schemes III and IV) were calculated from the steady-state kinetic expressions for this model described in Chen et al. (1987). This model assumes that the binding constants are pH independent, which has been demonstrated for *E. coli* DHFR (Fierke et al., 1987), and that proton transfer steps are fast. The isotope effect data were simulated by using an intrinsic isotope effect on hydride transfer of 3 as measured at high pH. Thus, Schemes III and IV can predict (within experimental error) all of the observed steady-state kinetic behavior, although the discrepancy in k_{cat}/K_M suggests that the estimation of the rate constant for binding H_2F to $E{\cdot}NH$ is low by a factor of 2. In addition, the internal equilibrium constant for hydride transfer, $K_{int} = 290$, can be scaled to the overall pH-independent equilibrium constant of $1.3 \times 10^{11}\ M^{-1}$ (Fierke et al., 1987) within experimental error where $K_{ov} = K_{int}(1/K_a)(K_4/K_2) = (5 \pm 4)$

$\times 10^{10}$ M^{-1} (Scheme V). The steady-state kinetic expressions for these schemes predict varying rate-limiting steps under a variety of conditions. Under k_{cat} conditions at low pH (<6), H_4F dissociation from E·NH·H_4F is mainly rate limiting while at high pH (>8) hydride transfer becomes solely rate limiting as evidenced by the large observed isotope effect. Under k_{cat}/K_M conditions at low pH, H_2F binding to E·NH is rate limiting, and at high pH, hydride transfer again becomes completely rate limiting. The apparent pK_a values characterizing the pH dependence of k_{cat} and k_{cat}/K_M are perturbed upward from the intrinsic pK_a of the ternary complex due to the nonequilibrium binding of H_2F (for k_{cat}/K_M) and to the change in rate-limiting steps (for k_{cat}).

Scheme V

$$E + H \underset{K_a}{\rightleftharpoons} H{\cdot}E + NH + H_2F \underset{K_2}{\rightleftharpoons} H{\cdot}E{\cdot}NH{\cdot}H_2F \overset{K_{int}}{\rightleftharpoons} E{\cdot}N{\cdot}H_4F \overset{K_4}{\rightleftharpoons} E + N + H_4F$$

The negative cooperativity in the binding of ligands in the E·H_4F·NADPH complex, implied by the preferential dissociation of H_4F, parallels that seen in our earlier NMR and binding studies at pH 6.8 on complexes with 5-formyl-H_4F (Birdsall et al., 1981). This tetrahydrofolate analogue was found to bind 600-fold less strongly in the ternary complex than in the binary complex, the weaker binding being due predominantly to an increase in its dissociation rate constant.

Folate Reduction by Wild-Type DHFR. *L. casei* DHFR catalyzes the reduction of folate to H_4F in two steps (Scheme VI) with hydride transfer occurring from the 4-*pro-R* position of NADPH to the *si* face of the pteridine in both cases (Charlton et al., 1979, 1985). Since the steady-state kinetic parameters for folate reduction (Table I) are much slower than any of the rate constants measured for H_2F reduction (Scheme III), the overall rate-limiting step must occur in reduction of folate to H_2F. The large isotope effect on k_{cat} suggests that under these conditions hydride transfer from NADPH to folate is rate limiting. The rate constant for hydride transfer may be faster than the observed k_{cat} if the active ternary substrate complex, E·Fol·NH, is in equilibrium with inactive ternary complexes (E·*Fol·NH) in which the folate is bound incorrectly as shown in Scheme VI. Birdsall et al. (1982, 1988, 1989) have observed "non-productive" conformational states in the E·$NADP^+$·Fol complex in which the pteridine ring of folate is bound in a similar manner to that of methotrexate. Therefore, the ratio of hydride transfer to H_2F compared to folate is at most 6000 (i.e., 430/0.075).

Scheme VI

$$E^{NH} + Fol \rightleftharpoons E^{NH}_{Fol} \rightleftharpoons E^{N}_{H_2Fol}$$
$$\downarrow\uparrow$$
$$E^{NH}_{*Fol}$$

W21L Mutant. The steady-state and binding kinetics for the W21L mutant suggest that the overall kinetic scheme has a similar form to that of wild type (Scheme III). Key features of this scheme include (i) NADPH and H_2F randomly bind to the enzyme to form the ternary complex, (ii) a favorable equilibrium exists for hydride transfer on the enzyme, (iii) dissociation of H_4F is fastest from the mixed ternary E·NH·H_4F complex so that the kinetic pathway for steady-state turnover at saturating substrate concentration follows a preferred pathway in which H_4F dissociation from DHFR occurs after NADPH replaces $NADP^+$, and (iv) the active ternary complex requires a protonated residue in the protein [presumably Asp-26 (Howell et al., 1986)]. Despite these similarities, many of the individual rate constants differ. First, the large deuterium isotope effect on steady-state turnover for W21L (Table I) suggests that hydride transfer, rather than H_4F dissociation, is rate limiting under these conditions. Thus, a major effect of this mutation is to decrease the rate constant for hydride transfer in both directions 100-fold (2.7 kcal/mol) with little or no effect on the equilibrium constant for hydride transfer. Second, the Trp to Leu substitution decreases binding in the coenzyme site with a larger effect on NADPH binding (≈3.5 kcal/mol) than $NADP^+$ binding (≈0.5 kcal/mol). This decrease in binding occurs mainly as an increase in the dissociation rate constant with little or no effect on the association rate constant. In addition, the mutation causes a smaller decrease in binding at the folate site mainly due to a decrease in the association rate constant. Finally, although the W21L mutation causes a decrease in the apparent pK_a values determined from steady-state turnover (Table I), it actually has little or no effect on the intrinsic pK_a of the ternary complex, E·NH·H_2F. The pK_a of 5.85 measured under k_{cat} conditions for W21L should reflect the intrinsic pK_a of the ternary complex (Chen et al., 1987) since hydride transfer is the rate-limiting step and the substrate dissociation rate constants are fast, while the apparent pK_a for wild-type DHFR (pK_a = 7.3) is higher than the true pK_a of 6.0 due to a change in rate-limiting steps as discussed above.

These results must be considered in terms of the *L. casei* DHFR protein structure. In the crystal structure of the *L. casei* DHFR·NADPH·MTX ternary complex (Bolin et al., 1982), Trp-21 is fairly close to both the coenzyme (3.9 Å from the Trp-21 C-2 proton to the amide nitrogen of NADPH) and inhibitor binding sites (4.6 and 4.7 Å from the indole NH of Trp-21 to the N1 proton and N8 of MTX) and also forms a hydrogen bond through a single water molecule to N8 of MTX. Thus, it is understandable that the W21L mutation would affect binding in both the coenzyme and folate sites. Birdsall et al. (1989) used a variety of one- and two-dimensional NMR techniques to compare the structure of W21L DHFR to wild type. They concluded that residues in the folate binding site and the adenosine region of the coenzyme binding site form the same ionic interactions and adopt essentially the same conformation. Furthermore, no large conformational changes in protein structure are observed, although small changes (≈0.2 Å) are seen at positions remote from the site of substitution. The major change observed is that the nicotinamide ring of the coenzyme binds differently. For example, in the case of the DHFR·$NADP^+$·trimethoprim ternary complex, the predominant conformation of $NADP^+$ is one in which the nicotinamide ring of the coenzyme is extended away from the enzyme structure and into the solvent (Birdsall et al., 1988), and the same appears to be true of binary complexes (Birdsall et al., unpublished results). While the reduced nicotinamide of bound NADPH does not extend into the solvent, it does bind differently in its complex with the W21L enzyme, its altered conformation offering an explanation for the decreased rate of hydride ion transfer. The marked difference in the effect of the substitution on the binding constants of NADPH and $NADP^+$ can be explained by the much smaller contribution of the oxidized nicotinamide ring to the overall binding (Birdsall et al., 1980).

Comparison of E. coli and L. casei DHFR. A comparison of the amino acid sequences of bacterial dihydrofolate reductases reveals a great deal of variation. For *E. coli* and *L. casei* DHFR, only 46 out of 162 residues are identical, a sequence homology of only 28%. The homology in the region

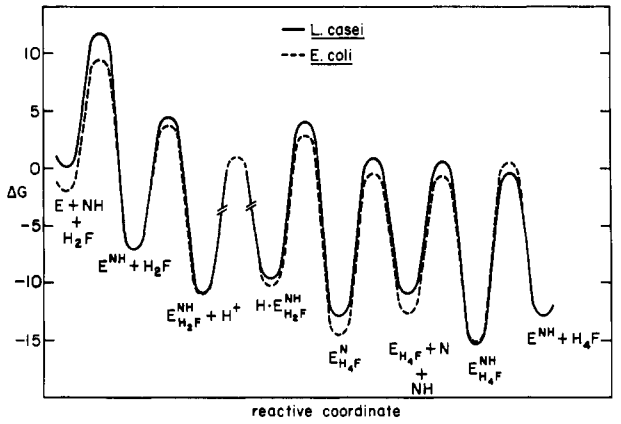

FIGURE 6: Gibbs free energy coordinate diagram for *E. coli* (---) and *L. casei* (—) dihydrofolate reductase aligned at the protonated substrate ternary complex, H·E·NH·H_2F, calculated at saturating ligand concentrations (1 mM), KMB buffer, pH 7.0, 25 °C.

of the active site is higher, >50%, calculated by comparing amino acids within 5 Å of MTX (Benkovic et al., 1988) and/or within 7 Å of NADPH (Benkovic et al., 1989). Nevertheless out of the 98 active-site residues implicated by these dimensions, some 36 are not identical. The tertiary structures of these two enzymes show a striking similarity (Bolin et al., 1982; Filman et al., 1982). Comparison of the total solvent-accessible surfaces of the active sites showed them to be within 7% of each other and the protein surfaces to be remarkably congruent despite being assembled from a mosaic of conserved and nonconserved residues (Benkovic et al., 1988, 1989). Moreover, several prominent changes in the active-site amino acids result in discernible differences in the positioning of the glutamate and benzoyl residues of bound MTX in the two enzymes.

Consistent with the similarities in protein–substrate interactions, the overall kinetic scheme of *L. casei* DHFR is identical in form with that of the *E. coli* enzyme. Several key features of these schemes (Scheme III; Fierke et al., 1987) are (i) the rate constant for steady-state turnover at low pH (≤6.5) is partially or completely limited by H_4F release, (ii) dissociation of H_4F is fastest from the mixed ternary complex, E·NH·H_4F, and (iii) the internal equilibrium constant for hydride transfer on the enzyme, K_{int}, is favorable [K_{int} = 1583 (EC); 290 (LC)].

In addition, the individual rate constants in the *L. casei* catalyzed reaction are remarkably similar to those in the *E. coli* reaction. Figure 6 is a reaction coordinate diagram comparing the steady-state turnover pathway for *E. coli* and *L. casei* DHFR, drawn at an arbitrary saturating substrate concentration (1 mM) at pH 7. We have lined up the two diagrams at the reactive ternary complex for comparison purposes. This diagram illustrates two main differences: (i) *L. casei* DHFR binds NADPH more tightly in both binary (E·NH, −2 kcal/mol) and ternary (E·NH·H_2F, −1.4 kcal/mol; E·NH·H_4F, −1.8 kcal/mol) complexes; and (ii) the internal equilibrium constant for hydride transfer is less favorable for *L. casei* DHFR (1 kcal/mol) due to both a decreased forward rate constant (2-fold) and an increased reverse rate constant (2.5-fold). These changes are smaller than those observed for single amino acid substitutions at the active site of DHFR such as that for *L. casei* W21L (Chen et al., 1987; Mayer et al., 1986; Howell et al., 1986; Fierke & Benkovic, 1988) despite the low amino acid homology between the two proteins. The virtual identity of the kinetic schemes despite variations in the active-site structure shows that the same catalytic surface can be constructed by differing combinations of amino acids.

Registry No. DHFR, 9002-03-3; NADPH, 53-57-6; H_2F, 4033-27-6; H_4F, 135-16-0; Fol, 59-30-3; TNADPH, 19254-05-8; $NADP^+$, 53-59-8; L-Trp, 73-22-3; L-Leu, 61-90-5; deuterium, 7782-39-0.

References

Andrews, J., Clore, G. M., Davies, R. W., Gronenborn, A. M., Gronenborn, B., Sims, P. F. G., & Stancombe, R. (1985) *Gene 35*, 217–222.

Barshop, B. A., Wreen, R. F., & Frieden, C. (1983) *Anal. Biochem. 130*, 134–145.

Benkovic, S. J., Fierke, C. A., & Naylor, A. M. (1988) *Science 239*, 1105–1110.

Benkovic, S. J., Adams, J. A., Fierke, C. A., & Naylor, A. M. (1989) *Pteridines 1*, 37–43.

Birdsall, B., Burgen, A. S. V., Rodrigues de Mirando, J., & Roberts, G. C. K. (1978) *Biochemistry 17*, 2102–2110.

Birdsall, B., Burgen, A. S. V., & Roberts, G. C. K. (1980) *Biochemistry 19*, 3723–3731.

Birdsall, B., Burgen, A. S. V., Hyde, E. I., Roberts, G. C. K., & Feeney, J. (1981) *Biochemistry 20*, 7186–7195.

Birdsall, B., Gronenborn, A., Hyde, E. I., Clore, G. M., Roberts, G. C. K., Feeney, J., & Burgen, A. S. V. (1982) *Biochemistry 21*, 5831–5838.

Birdsall, B., King, R. W., Wheeler, M. R., Lewis, C. A., Jr., Goode, S. R., Dunlap, R. B., & Roberts, G. C. K. (1983) *Anal. Biochem. 132*, 353–361.

Birdsall, B., DeGraw, J., Feeney, J., Hammond, S., Searle, M. S., Roberts, G. C. K., Colwell, W. T., & Crase, J. (1988) *FEBS Lett. 217*, 106–110.

Birdsall, B., Andrews, J., Ostler, G., Tendler, S. J. B., Feeney, J., Roberts, G. C. K., Davies, R. W., & Cheung, H. T. A. (1989) *Biochemistry 28*, 1353–1362.

Bolin, J. T., Filman, D. J., Matthews, D. A., Hamlin, R. C., & Kraut, S. (1982) *J. Biol. Chem. 257*, 13650–13662.

Cayley, P. J., Dunn, S. M. J., & King, R. W. (1981) *Biochemistry 20*, 874–879.

Charlton, P. A., Young, D. W., Birdsall, B., Feeney, J., & Roberts, G. C. K. (1979) *J. Chem. Soc., Chem. Commun.*, 922–924.

Charlton, P. A., Young, D. W., Birdsall, B., Feeney, J., & Roberts, G. C. K. (1985) *J. Chem. Soc., Perkin Trans. 1*, 1349–1353.

Chen, J.-T., Taira, K., Tu, C.-P., & Benkovic, S. J. (1987) *Biochemistry 26*, 4093–4100.

Curthoys, H. P., Scott, J. M., & Rabinowitz, S. C. (1972) *J. Biol. Chem. 247*, 1959–1964.

Dann, J. G., Ostler, G., Bjur, R. A., King, R. W., Scudder, P., Turner, P. C., Roberts, G. C. K., Burgen, A. S. V., & Harding, N. G. L. (1976) *Biochem. J. 157*, 559–571.

Dawson, R. M. C., Elliott, D. C., Elliott, W. H., & Jones, K. M. (1969) *Data for Biochemical Research*, Oxford University Press, Oxford, U.K.

Dunn, S. M. J., & King, R. W. (1980) *Biochemistry 19*, 766–773.

Dunn, S. M. J., Batchelor, J. G., & King, R. W. (1978) *Biochemistry 17*, 2356–2364.

Dyson, R. D., & Eisenberg, I. (1971) *Biochemistry 10*, 3233–3241.

Ellis, K. J., & Morrison, J. F. (1982) *Methods Enzymol. 87*, 405–426.

Fierke, C. A., & Benkovic, S. J. (1989) *Biochemistry 28*, 478–486.

Fierke, C. A., Johnson, K. A., & Benkovic, S. J. (1987) *Biochemistry 26*, 4085–4092.

Howell, E. E., Villafranca, J. E., Warren, M. S., Oakley, S. J., & Kraut, J. (1986) *Science 231*, 1123–1128.

Howell, E. E., Warren, M. S., Booth, C. L. J., Villafranca, C. E., & Kraut, J. (1987) *Biochemistry 26*, 8591–8598.
Hyde, E. I. (1981) Ph.D. Thesis.
Johnson, K. A. (1986) *Methods Enzymol. 134*, 677–705.
Kallen, R. G., & Jencks, W. P. (1966) *J. Biol. Chem. 241*, 5845–5850.
Kramer, W., Drutsas, V., Jansen, H. W., Kramer, B., Pflugfelder, M., & Fritz, H.-J. (1984) *Nucleic Acids Res. 12*, 9441–9456.
Lakowicz, J. R. (1983) *Principles of Fluorescence Spectroscopy*, Plenum Press, New York.
Mathews, C. K., & Huennekens, F. M. (1963) *J. Biol. Chem. 235*, 3304–3308.
Matthews, D. A., Bolin, J. T., Burridge, J. M., Filman, D. J., Valz, K. W., Kaufman, B. T., Beddell, C. R., Champness, J. N., Stammer, D. K., & Kraut, J. (1985) *J. Biol. Chem. 260*, 381–391.
Mayer, R. J., Chen, J.-T., Taira, K., Fierke, C. A., & Benkovic, S. J. (1986) *Proc. Natl. Acad. Sci. U.S.A. 83*, 7718–7720.
Orr, G. A., & Blanchard, J. S. (1984) *Anal. Biochem. 142*, 232–234.
Penner, M. H., & Frieden, C. (1985) *J. Biol. Chem. 260*, 5366–5369.
P-L Biochemicals (1961) Circular OR-18, P-L Biochemicals, Milwaukee, WI.
Rabinowitz, J. C. (1960) *Enzymes, 2nd Ed. 2*, 185–252.
Roth, B., & Strelitz, J. Z. (1969) *J. Org. Chem. 34*, 821–836.
Seeger, D. R., Cosulich, D. B., Smith, J. M., & Hultquist, M. E. (1949) *J. Am. Chem. Soc. 71*, 1753–1758.
Smith, G. K., Benkovic, P. A., & Benkovic, S. J. (1981) *Biochemistry 20*, 4034–4036.
Stone, S. R., & Morrison, J. F. (1982) *Biochemistry 21*, 3757–3765.
Stone, S. R., & Morrison, J. F. (1984) *Biochemistry 23*, 2753–2758.

EPR and Kinetic Analysis of the Interaction of Halides and Phosphate with Nitrate Reductase†

Christopher J. Kay and Michael J. Barber*

Department of Biochemistry and Molecular Biology, University of South Florida College of Medicine, Tampa, Florida 33612

Received January 10, 1989; Revised Manuscript Received April 12, 1989

ABSTRACT: Electron paramagnetic resonance spectra obtained during turnover of the Mo center of NADH:nitrate reductase at pH 8 were comprised of two Mo(V) species, signal A (g_1 = 1.996, g_2 = 1.969, g_3 = 1.967, A_1^H = 1.25 mT, A_2^H = 1.18 mT, and A_3^H = 1.63 mT) and signal B (g_1 = 1.996, g_2 = 1.969, and g_3 = 1.967), the former exhibiting superhyperfine interaction due to strong coupling with a single, exchangeable proton. Binding of halides and nitrite to the Mo center increased the proportion of signal A whereas phosphate had no effect on the EPR line shape. Halides decreased and phosphate increased the rates of enzyme activities involving the Mo center (NADH:nitrate reductase and reduced methyl viologen:nitrate reductase), but neither had any effect on activities involving FAD (NADH:ferricyanide reductase) or heme (NADH:cytochrome *c* reductase), indicating specific binding of halides to the Mo center. Halides were found to be weak, mixed competitive–noncompetitive inhibitors (Cl^- K_I = 39 mM, μ = 0.2 M, pH 8) of nitrate reductase forming a catalytically inactive ternary halide–nitrate–enzyme complex. Inhibition patterns changed from nearly noncompetitive (F^-) to nearly competitive (I^-). The weakening of nitrate binding due to halide binding correlated with increased halide electronegativity rather than ionic radius. In contrast, phosphate (K_d = 7.4 mM, μ = 0.2 M, pH 8) and arsenate were determined to be nonessential activators, characterized by a constant value of $(V_{max}/K_m)_{app}$, increasing nitrate reductase activity by weakening nitrate binding without affecting the stability of the transition state. Phosphate had no effect on product inhibition by nitrite (K_I = 0.33 mM) or the oxidation–reduction midpoint potentials of the Mo center.

Assimilatory nitrate reductase (NR)[1] from *Chlorella vulgaris* is a homotetrameric enzyme of molecular weight 375K, containing FAD, heme, and Mo–pterin prosthetic groups in a ratio of 1:1:1 per subunit (Giri & Ramadoss, 1979; Howard & Solomonson, 1982). The enzyme catalyzes the initial and regulated step in the assimilation of nitrate, the NADH-dependent reduction of nitrate to nitrite (Guerrero et al., 1981; Dunn-Coleman et al., 1984). The Mo prosthetic group of NR is the site of nitrate reduction and is complexed to a sulfur-containing pterin derivative (molybdopterin) (Johnson et al.,

† This work was supported by Grant GM32696 from the National Institutes of Health, Grant 88-37120-3871 from the U.S. Department of Agriculture, and Grant DCB-8615836 from the National Science Foundation.

* Address correspondence to this author at the Department of Biochemistry and Molecular Biology, University of South Florida, MDC Box 7, Tampa, FL 33612.

[1] Abbreviations: NR, nitrate reductase; EPR, electron paramagnetic resonance; EXAFS, X-ray absorption fine structure; NADH:NR, NADH-dependent nitrate reductase; NADH:FR, NADH-dependent ferricyanide reductase; NADH-CR, NADH-dependent cytochrome *c* reductase; FH_2:NR, reduced FMN-dependent nitrate reductase; MV:NR, reduced methyl viologen dependent nitrate reductase.

0006-2960/89/0428-5750$01.50/0